

Resonant modes in strain-induced graphene superlattices

F. M. D. Pellegrino,^{1,2} G. G. N. Angilella,^{1,2,3,4} and R. Pucci^{1,2}

¹*Dipartimento di Fisica e Astronomia, Università di Catania, Via S. Sofia, 64, I-95123 Catania, Italy*

²*CNISM, UdR di Catania, I-95123 Catania, Italy*

³*Scuola Superiore di Catania, Università di Catania, Via Valdisavoia, 9, I-95123 Catania, Italy*

⁴*INFN, Sezione di Catania, I-95123 Catania, Italy*

We study tunneling across a strain-induced superlattice in graphene. In studying the effect of applied strain on the low-lying Dirac-like spectrum, both a shift of the Dirac points in reciprocal space, and a deformation of the Dirac cones is explicitly considered. The latter corresponds to an anisotropic, possibly non-uniform, Fermi velocity. Along with the modes with unit transmission usually found across a single barrier, we analytically find additional resonant modes when considering a periodic structure of several strain-induced barriers. We also study the band-like spectrum of bound states, as a function of conserved energy and transverse momentum. Such a strain-induced superlattice may thus effectively work as a mode filter for transport in graphene.

PACS numbers: 81.05.ue, 72.80.Vp, 85.30.Mn

Graphene is a single layer of carbon atoms in the sp^2 hybridization state, arranged according to a honeycomb lattice^{1,2}. Transport properties in graphene are largely determined by its reduced dimensionality, which characterizes its remarkable electronic properties^{3,4}. These include low-energy quasiparticles with a Dirac-like spectrum and a linearly vanishing density of states (DOS) at the Fermi level. Evidence of such an unconventional behaviour is to be found in several electronic properties, such as Klein tunneling⁵⁻⁹, the optical conductivity¹⁰⁻¹², and the plasmon dispersion relation¹³⁻¹⁶. These have been predicted to depend quite generally on applied strain¹⁷, following the earlier suggestion that suitably deformed graphene sheets could be engineered into nanodevices with the desired electron properties¹⁸. For instance, it has been recently demonstrated that the electrical properties of epitaxial graphene on SiC strongly depend on the local strain induced in graphene by the substrate¹⁹. One thus expects that a suitable pattern of periodically repeating stripes, with alternating values of strain, *i.e.* a strain-induced superlattice, may produce coherent effects on single particle transport, depending on the energy and momentum of the incident electrons. Here, we therefore study the possible occurrence of resonant states within a strain-induced superlattice in graphene.

We consider quasiparticle transmission across N identical barriers, each of width ℓ , the inter-barrier separation being also ℓ , such that $2N\ell = D$ (Fig. 1). Let x denote the coordinate orthogonal to the barriers, forming an angle θ with the graphene zig-zag direction. Thus, $\theta = 0$ (*resp.*, $\theta = \pi/2$) will refer to a superlattice oriented along the zig-zag (*resp.*, armchair) direction. Such a superlattice is usually obtained via a step-wise varying gate potential $U(x) = U_{\pm}$, with $U(x) = U_-$ within each barrier [$2(m-1)\ell \leq x \leq 2m\ell$, $m = 1, \dots, N$], and $U(x) = U_+$ between two neighboring barriers [$(2m-1)\ell \leq x \leq 2m\ell$, $m = 1, \dots, N$]. Here, we will additionally consider a nonuniform profile of uniaxial strain $\varepsilon = \varepsilon(x)$ applied along the θ direction, with strain modulus alternating

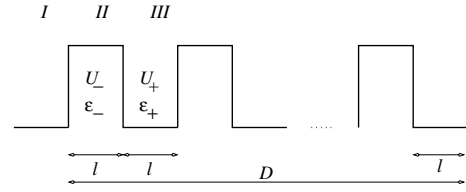


FIG. 1: Schematic plot of the superlattice of N identical barriers, with ℓ denoting both each barrier's width and the inter-barrier separation, while $D = 2N\ell$. Subscript $-$ refers to the region within a barrier (labelled II), while subscript $+$ refers to the interbarrier region (labelled I and III).

between the values $\varepsilon(x) = \varepsilon_{\pm}$ inside and outside a barrier, as above. Such a dependence approximates a smooth periodic strain wave with period 2ℓ , as a train of sharp steps.

Within each barrier, strain is described by the tensor $\varepsilon = \frac{1}{2}\varepsilon[(1-\nu) + (1+\nu)A(\theta)]$, where $\varepsilon = \varepsilon(x)$ is the strain modulus, $\nu = 0.14$ is Poisson's ratio for graphene²⁰, and $A(\theta) = \cos(2\theta)\sigma_z + \sin(2\theta)\sigma_x$, with σ_i ($i = x, y, z$) denoting the Pauli matrices. Within a quite general tight-binding approach³, strain then enters the electronic properties through the dependence of the hopping parameters on the lattice vectors²¹. Expanding such a tight-binding Hamiltonian to linear order in the strain modulus, one finds that the low-lying spectrum can still be described by a Dirac-like Hamiltonian, but now (i) applied strain shifts the location of the Dirac points in reciprocal space with respect to $\pm\mathbf{K}$ at the vertices of the first Brillouin zone, and (ii) it induces a deformation of the Dirac cones, which can be accounted in terms of an anisotropic Fermi velocity v_F . Specifically, one finds for the Hamiltonian under applied strain

$$H = \hbar v_F \mathcal{U}^\dagger(\theta) \tilde{\sigma} \cdot \mathbf{q} \mathcal{U}(\theta), \quad (1)$$

where $\mathbf{q} = (q_1, q_2)^\top$ measures the wave vector displacement from the shifted Dirac points $\mathbf{q}_{Da} = \pm(\kappa_0\varepsilon(1 + \nu)\cos(2\theta), -\kappa_0\varepsilon(1 + \nu)\sin(2\theta))^\top$, $\tilde{\sigma}_i = (1 - \lambda_i\varepsilon)\sigma_i$ ($i =$

1,2) take into account of the strain-induced deformation of the Fermi velocity, with $\lambda_x = 2\kappa$, $\lambda_y = -2\kappa\nu$, $\mathcal{U}(\theta) = \text{diag}(1, e^{-i\theta})$ is the unitary matrix performing a rotation mapping the zig zag direction onto the the direction x of applied strain, $\kappa_0 = (a/2t)|\partial t/\partial a| \approx 1.6$ is related to the logarithmic derivative of the nearest-neighbor hopping parameter t with respect to the lattice parameter a at zero strain, and $\kappa = \kappa_0 - \frac{1}{2}$ (cf. Ref. 22).

Since the strain superlattice is uniform along the coordinate orthogonal to the direction of applied strain, say y , stationary eigenmodes will be characterized by constant energy E and transverse wave vector k_y . The stationary Dirac equation associated to Eq. (1), with appropriate matching conditions for the quasiparticle spinor due to the continuity of its associated current density at the barriers' edges, can then be equivalently recast using the transfer matrix formalism^{23,24}. Following Ref. 17, for the transfer matrix across the first, say, barrier in Fig. 1, one finds $\mathbb{M}^{(1)}(2\ell, 0) = e^{iq_{Dx}^{(0)}(\varepsilon_+ + \varepsilon_-)\ell} \tilde{\mathbb{M}}^{(1)}$, where $\mathbf{q}_D^{(0)} = \mathbf{q}_D(\varepsilon = 1)$, and $\tilde{\mathbb{M}}^{(1)}$ is a unimodular matrix, $\det \tilde{\mathbb{M}}^{(1)} = 1$. Specifically, one obtains

$$\tilde{\mathbb{M}}_{11}^{(1)} = \lambda + i\eta, \quad (2a)$$

$$\lambda = \frac{\sinh(q_- \ell) \sinh(q_+ \ell)}{q_- q_+} (\kappa_- \kappa_+ - u_- u_+) + \cosh(q_- \ell) \cosh(q_+ \ell), \quad (2b)$$

$$\eta = i \left[\frac{u_+ u_- - \kappa_+ \kappa_-}{q_+ q_-} \sinh(q_- \ell) \cosh(q_+ \ell) - \sinh(q_+ \ell) \cosh(q_- \ell) \right], \quad (2c)$$

where λ is always real, whereas η can be real or purely imaginary, depending k_y and E . More compactly, one also finds

$$\tilde{\mathbb{M}}_{11}^{(1)} = \exp(q_+ \ell) \left[\frac{\kappa_+ \kappa_- - u_+ u_-}{q_+ q_-} \sinh(q_- \ell) + \cosh(q_- \ell) \right]. \quad (3)$$

In Eqs. (2) and (3), we have employed the definitions $\kappa_{\pm} = (1 - \lambda_y \varepsilon_{\pm})(k_y - q_{Dy}^{(0)} \varepsilon_{\pm}) / (1 - \lambda_x \varepsilon_{\pm})$, $u_{\pm} = (E - U_{\pm}) / [\hbar v_F (1 - \lambda_x \varepsilon_{\pm})]$, and $q_{\pm} = \sqrt{\kappa_{\pm}^2 - u_{\pm}^2}$. Making use of the Chebyshev identity for the N th power of a unimodular matrix²⁵, for the evolution matrix across N identical barriers, one finds²²

$$[\tilde{\mathbb{M}}^{(1)}]_{11}^N = \frac{\sinh(Nz)}{\sinh z} \tilde{\mathbb{M}}_{11}^{(1)} - \frac{\sinh((N-1)z)}{\sinh z}, \quad (4)$$

where $\cosh z = \lambda$. Finally, the transmission can be related to the evolution matrix as

$$T_N(E, k_y) = \left| [\tilde{\mathbb{M}}^{(1)}]_{11}^N \right|^{-2}. \quad (5)$$

We are now in the position to discern whether an electronic mode is characterized by an oscillating or evanescent behavior far from the barrier superlattice. To this aim, we preliminarily observe that, depending on E and

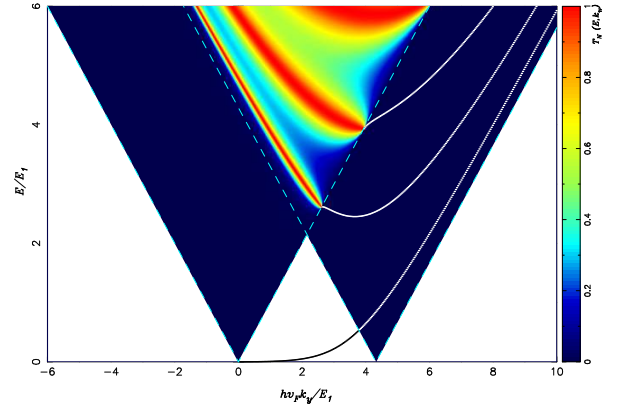


FIG. 2: (Color online) Single electron transmission $T_1(E, k_y)$, Eq. (5) across a single barrier ($N = 1$, $\ell = 25$ nm), as a function of scaled transverse wave vector $\hbar v_F k_y / E_1$ and scaled energy E / E_1 , Eq. (6), with $E_1 \approx 40$ meV. Here, strain is applied along the armchair direction, $\theta = \pi/2$, and we set $\varepsilon_- = 0.02$, $\varepsilon_+ = 0$, and $U_{\pm} = 0$. Cyan dashed lines delimit cones corresponding to the (deformed) Dirac cones outside (left cone) and within (right cone) the barrier (regions I+III and II, respectively, in Fig. 1). Solid lines outside the left Dirac cone correspond to bound modes.

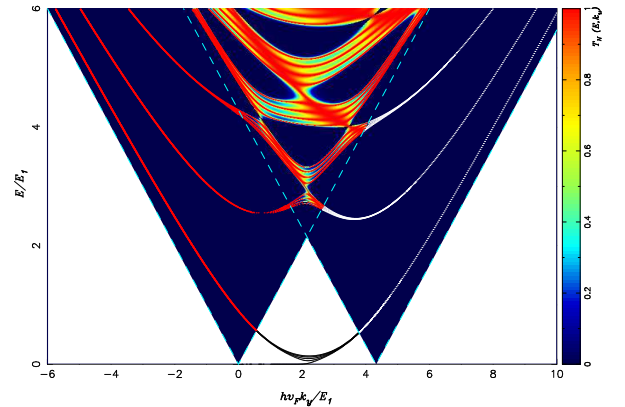


FIG. 3: (Color online) Single electron transmission $T_5(E, k_y)$, Eq. (5) across a superlattice of $N = 5$ identical barriers (Fig. 1), as a function of scaled transverse wave vector $\hbar v_F k_y / E_1$ and scaled energy E / E_1 , Eq. (6). All other parameters are as in Fig. 2. Red lines outside the right cone correspond to resonant modes.

k_y , one has a propagating (*resp.*, evanescent) wave for $q_{\pm}^2 < 0$ (*resp.*, $q_{\pm}^2 > 0$), where the subscript $+$ refers to the region between two consecutive barriers $[(2m-1)\ell \leq x \leq 2m\ell, m = 1, \dots, N]$, and the subscript $-$ refers to the region within a barrier $[2(m-1)\ell \leq x \leq (2m-1)\ell, m = 1, \dots, N]$ (Fig. 1).

Fig. 2 shows the single electron transmission $T_N(E, k_y)$ across a single barrier, Eq. (5) with $N = 1$, as a function of the transverse wave vector $\hbar v_F k_y / E_1$ and energy E / E_1 , each scaled by the characteristic energy

$$E_1 = \frac{\pi \hbar v_F}{2\ell \gamma}, \quad (6)$$

where $\gamma = \frac{1}{2}[(1-\lambda_x\varepsilon_+)^{-1} + (1-\lambda_x\varepsilon_-)^{-1}]$. Here and in the following, strain is applied along the armchair direction, $\theta = \pi/2$, and we set $\varepsilon_- = 0.02$, $\varepsilon_+ = 0$, and $U_{\pm} = 0$. In Fig. 2, cyan dashed lines delimit the two (deformed) Dirac cones defined by $q_+^2 < 0$ (left cone) and $q_-^2 < 0$ (right cone), corresponding to regions I+III and II in Fig. 1), respectively. One finds that $T_1(E, k_y)$ is defined within the left cone and is exponentially vanishing within the intersection between both cones. This corresponds to having propagating modes in all the three regions. In this case, resonant modes, *i.e.* propagating modes with unit transmission, are characterized by the condition for stationary waves

$$\tilde{q}_-\ell = m\pi, \quad (7)$$

where $q_- = i\tilde{q}_-$, and m is an integer.

Fig. 3 shows the single electron transmission $T_N(E, k_y)$ across a superlattice composed of five identical barriers, Eq. (5) with $N = 5$. Again, nonzero values of the transmission are to be found within the intersection of the Dirac cones corresponding to the region inside a barrier and between two consecutive barriers. However, at variance of the case $N = 1$, because of multiple scatterings, a nonzero transmission is also possible beyond the cone $q_-^2 < 0$. This corresponds to having evanescent modes within the barriers. Such a phenomenon is analogous to what happens to photons propagating across a 1D photonic crystal with alternative layers of a left-handed and a right-handed material (1D metamaterial)²⁶. As for resonant modes, $T_N(E, k_y) = 1$, besides the ones given by Eq. (7) regardless of N , additional resonant modes are given by the condition

$$\lambda = \cos\left(\frac{\pi j}{N}\right), \quad j = 1, \dots, N-1, \quad (8)$$

where λ is defined by Eq. (2b), and $|\lambda| < 1$. The latter condition implies that these resonant modes have globally propagating behavior. Comparing Figs. 2 and 3, one finds that, in the domain within both Dirac cones, in addition to the resonant modes given by Eq. (7), in the case $N > 1$ there exist $N - 1$ new resonant modes given

by Eq. (8). It should also be noted that in the domain within the left cone but outside the second the resonant modes, which are only given by Eq. (8), are characterized by quite narrow lines in the transmission plots.

Outside the left Dirac cone, it is still possible to find bound states^{18,27,28}. Within the transfer matrix method, these are given by the condition²⁹ $[\mathbb{M}^{(1)}]_{11}^N = 0$. For $q_+^2 > 0$ one finds evanescent modes outside the barriers, and therefore also far from the superlattice structure. In the case $N = 1$, one finds several such confined modes within the second cone (Fig. 2, solid lines outside the left cone), whereof only one such mode survives in the region outside both cones. The latter is the surface mode analyzed in Ref. 18. In the case $N > 1$ (Fig. 3, solid lines outside the right cone), one finds that to each bound mode in the single barrier case there correspond exactly N bound states outside either cones. This is remindful of electron bands in solids, where the overlap of N periodically arranged atomic orbitals give rise to a band of N states.

In conclusion, we have found that a strain-induced superlattice in graphene can accommodate additional resonant quasiparticle states, analytically characterized by Eq. (8), besides the ones usually found across a single barrier, given by Eq. (7). One finds that applied strain modifies the kinetic part of the quasiparticle Hamiltonian, which preserves its Dirac-like character, but around shifted and deformed Dirac cones. This can be described in terms of a coordinate-dependent, periodic, profile of the Fermi velocity, which produces coherent effects on the quasiparticle transmission. Specifically, we find resonant modes with globally propagating behavior far from the superlattice, for conserved energy and transverse momentum within the intersection of the two deformed Dirac cones corresponding to the two alternating strained regions. Other modes are exponentially suppressed, and we also discuss the spectrum of bound states, which arrange themselves as ‘bands’, depending on the overall number of barriers making up the superlattice. We thus surmise that a strain-induced superlattice in graphene can be used as a filter for the resonant modes here discussed.

¹ K. S. Novoselov, A. K. Geim, S. V. Morozov, D. Jiang, Y. Zhang, S. V. Dubonos, I. V. Grigorieva, and A. A. Firsov, *Science* **306**, 666 (2004).

² K. S. Novoselov, A. K. Geim, S. V. Morozov, D. Jiang, M. I. Katsnelson, I. V. Grigorieva, S. V. Dubonos, and A. A. Firsov, *Nature* **438**, 197 (2005).

³ A. H. Castro Neto, F. Guinea, N. M. R. Peres, K. S. Novoselov, and A. K. Geim, *Rev. Mod. Phys.* **81**, 000109 (2009).

⁴ D. S. L. Abergel, V. Apalkov, J. Berashevich, K. Ziegler, and T. Chakraborty, *Adv. Phys.* **59**, 261 (2010).

⁵ J. M. Pereira, V. Mlinar, F. M. Peeters, and P. Vasilopoulos, *Phys. Rev. B* **74**, 045424 (2006).

⁶ M. Barbier, P. Vasilopoulos, and F. M. Peeters, *Phys. Rev. B* **80**, 205415 (2009).

⁷ M. Barbier, P. Vasilopoulos, and F. M. Peeters, *Phys. Rev. B* **81**, 075438 (2010).

⁸ M. Barbier, P. Vasilopoulos, and F. M. Peeters, *Phys. Rev. B* **82**, 235408 (2010).

⁹ N. M. R. Peres, *J. Phys.: Cond. Matter* **21**, 323201 (2009).

¹⁰ F. Wang, Y. Zhang, C. Tian, C. Girit, A. Zettl, M. Crommie, and Y. R. Shen, *Science* **320**, 206 (2008).

¹¹ T. Stauber, N. M. R. Peres, and A. K. Geim, *Phys. Rev. B* **78**, 085432 (2008).

¹² F. M. D. Pellegrino, G. G. N. Angilella, and R. Pucci, *Phys. Rev. B* **81**, 035411 (2010).

- ¹³ E. H. Hwang and S. Das Sarma, Phys. Rev. B **75**, 205418 (2007).
- ¹⁴ S. H. Abedinpour, G. Vignale, A. Principi, M. Polini, W.-K. Tse, and A. H. MacDonald, Phys. Rev. B **84**, 045429 (2011), URL <http://link.aps.org/doi/10.1103/PhysRevB.84.045429>.
- ¹⁵ F. M. D. Pellegrino, G. G. N. Angilella, and R. Pucci, Phys. Rev. B **82**, 115434 (2010).
- ¹⁶ F. M. D. Pellegrino, G. G. N. Angilella, and R. Pucci, High Press. Res. **31**, 98 (2011).
- ¹⁷ F. M. D. Pellegrino, G. G. N. Angilella, and R. Pucci, Phys. Rev. B **84**, 195407 (2011).
- ¹⁸ V. M. Pereira and A. H. Castro Neto, Phys. Rev. Lett. **103**, 046801 (2009).
- ¹⁹ T. Low, V. Perebeinos, J. Tersoff, and P. Avouris, Phys. Rev. Lett. **108**, 096601 (2012), URL <http://link.aps.org/doi/10.1103/PhysRevLett.108.096601>.
- ²⁰ M. Farjam and H. Rafii-Tabar, Phys. Rev. B **80**, 167401 (2009).
- ²¹ V. M. Pereira, A. H. Castro Neto, and N. M. R. Peres, Phys. Rev. B **80**, 045401 (2009).
- ²² F. M. D. Pellegrino, G. G. N. Angilella, and R. Pucci, Phys. Rev. B **84**, 195404 (2011).
- ²³ M. Titov, Eur. Phys. Lett. **79**, 17004 (2007).
- ²⁴ H. Bruus and K. Flensberg, *Many-Body Quantum Theory in Condensed Matter Physics: An Introduction* (Oxford University Press, Oxford, 2004).
- ²⁵ P. Yeh, A. Yariv, and C. Hong, J. Opt. Soc. Am. **67**, 423 (1977).
- ²⁶ L. Wu, S. He, and L. Shen, Phys. Rev. B **67**, 235103 (2003).
- ²⁷ M. Ramezani Masir, P. Vasilopoulos, and F. M. Peeters, New J. Phys. **11**, 095009 (2009).
- ²⁸ M. Barbier, P. Vasilopoulos, and F. M. Peeters, Phil. Trans. R. Soc. A **368**, 5499 (2010).
- ²⁹ Y. P. Bliokh, V. Freilikher, and F. Nori, Phys. Rev. B **81**, 075410 (2010), URL <http://link.aps.org/doi/10.1103/PhysRevB.81.075410>.